

A MECHANISM FOR CREATING VARIABLE NANOMETER GAPS

Hongshen Ma¹ and Alexander H. Slocum²

¹Department of Electrical Engineering and Computer Science,

²Department of Mechanical Engineering,
Massachusetts Institute of Technology
Cambridge, MA, USA

INTRODUCTION

The creation and control of electrodes separated by a nanometer gap can provide a direct method to interface with materials and phenomenon on the size-scale of individual molecules. In particular, the study of electrokinetic properties of liquids within nanogaps may enable new measurement modalities for determining the molecular structure and composition of materials. As discussed by the theoretical work of Bazant et al [1] and demonstrated by the experimental work of Yi et al [2], the electrical impedance of fluid in nanometer channels can be dramatically different from values predicted by traditional macroscale models. When the physics of these situations are completely understood, it may be possible to apply these techniques to (1) industrial chemical processes to detect the presence of certain molecules in solution; (2) biochemical research to determine the electromechanical properties of biological molecules; and (3) molecular-electronics research to measure the electron transport properties of molecules and nanostructures. This paper reports on the development of an experimental apparatus for studying the electrokinetic properties of liquid thin films in an extremely confined state. In particular, this apparatus will act as an impedance measurement instrument where the distance between electrodes can be varied.

While a number of previous studies have demonstrated methods to create nanogap electrodes with fixed geometries using nano- and micro-fabrication technologies [3-5], few have investigated designs for a variable spacing nanogap [6]. This capability is particularly desired in electrical impedance measurements since measurement parasitics can be effectively removed by repeated measurements at different gap spacing. Furthermore, in some instances the electromechanical properties of the fluid are strongly affected by the nanoscale geometry of the gap, the electrode separation can therefore be used as a parameter to study these effects.

APPROACH

The most straightforward approach to creating electrodes separated by a variable nanometer gap is to develop a mechanism that brings together nanometer smooth, planar electrodes in a parallel manner. For example, one such mechanism, known as the Nanogate was designed as a nanoscale fluid valve [7]. As an impedance measurement cell, however, the implementation of such a design can be extremely difficult since minute non-parallelism between surfaces used to define a nanometer gap can cause the electrodes to short-circuit together, thereby altogether bypassing the fluid impedance.

The non-parallelism problem can be avoided by using spherical electrodes instead of planar electrodes. Since tangent planes through the closest points between two spheres are always parallel to each other, a small gap between two spheres approximates a small gap between two perfectly parallel planar surfaces. As long as the spheres have a smooth enough surface quality, this approximation can be improved by enlarging the diameter of the spheres. Commercially available spheres used for ball bearings and precision alignment equipment can be produced with extremely smooth surface quality. For example, a typical silicon-wafer has an RMS surface roughness of 1nm while a typical production polished tungsten carbide ball has an RMS surface roughness of 5nm. Even better surface finish can be found on balls made of specialty materials such as silicon nitride, borosilicate glass, and ruby.

A second approach to resolving the non-parallelism problem is to use the spherical electrode as a master to emboss a soft metal to create a complementary shape to the starting spherical surface. The nanogap is formed as the master sphere is pulled back precisely from its mating surface. By taking advantage of the large Hertzian stresses generated by the master sphere and choosing the proper substrate material, the deformation can be almost entirely

plastic with minimal elastic spring back. Figure 1 shows the surface profile of a tungsten carbide ball and the embossed surface in pure aluminum. The embossing process removed much of the “hills”, but kept the “valleys” intact.

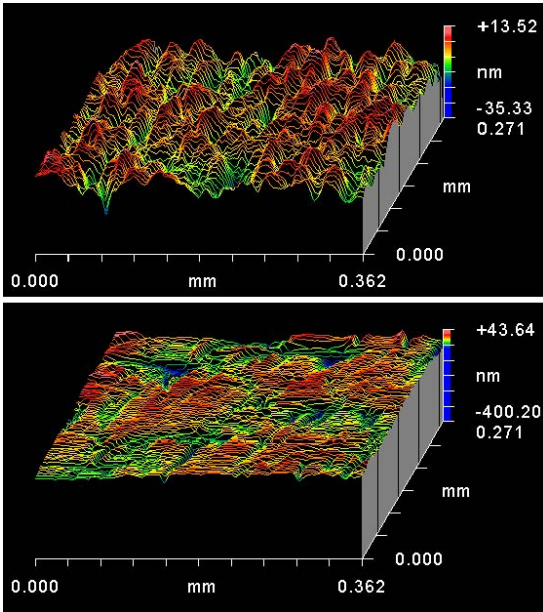


Figure 1: Surface profiles of a tungsten carbide ball (top) and the embossed pure aluminum surface (bottom). RMS roughness values are 5nm and 14nm respectively.

Both the two-spheres and the embossing approach have their advantages and drawbacks. The two-spheres approach is simple and does not require an extremely high degree of actuator reproducibility. However, a relatively larger sample volume is required because of the geometry of the impedance cell. The embossing approach requires a smaller sample volume, but is mechanically more demanding since large forces are required during the initial embossing process while the subsequent low-force return motion must follow same path precisely. The mechanism designed in this paper is amenable to both configurations. Further development work focuses on the two spheres approach, which can also be actuated using a direct piezoelectric actuator.

MECHANISM DESIGN

The mechanism described in this paper is designed to experiment with both the two-spheres and embossed configurations. The primary functional requirements of this mechanism include nanometer control of position, absolute repeatability of motion, ability to apply forces up to 2000 Newtons, and

minimal noise and drift of the gap distance. A simple mechanism that fulfills such requirements is a cantilever connected by a flexural hinge.

Flexural Hinge

The cartwheel flexure, indicated as flexure 1 in Figure 2, is one type of flexural hinge with a large travel and load capacity.

The maximum stress of the cartwheel flexure can be expressed as,

$$\sigma_{\max} = \frac{E\alpha t}{L},$$

where α is the deflection angle of the flexure; L is the length of both the vertical and horizontal flexure beams; t is the thickness of the flexure; and E is the elastic modulus.

Course Actuator

The position of the cantilever beam is controlled by course and fine manual adjusters. The course adjuster is a 1/4"-80 lead screw (Thorlabs: FS25AB200) that pushes near the end of the cantilever beam to achieve a 3:1 reduction at the sample position. The lead screw advances 0.3mm per revolution. Assuming 1 degree angular resolution is achievable by hand, a position resolution of 0.3um can be achieved at the electrode. Backlash in the lead screw is eliminated by an anti-backlash bushing, supplied with the lead screw. The tip of the lead screw is a ball which pushes into a carbide cup (Bird Precision: RB-25009). The radius of the carbide cup is greater than that of the ball tip in order to insure a consistent point of contact.

The effects of parasitic motion from the course actuator in both x- and y-axes are reduced by a flexible carriage as shown in Figure 2. Thin vertical flexures act like a wobble pin and allow the carriage mechanism to be flexible along the x-axis which reduces the mechanical coupling from the lead screw to the main cantilever beam. The same type of flexibility can be realized along the y-axis by thinning the flexure beams. The effect of parasitic motion along the y-axis is further reduced by flexure 2, which increases the stiffness of the main beam in that direction.

Fine Actuator

The fine actuator works in series with the course actuator by deflecting flexure 3. The fine actuator is a precision differential screw that can operate in both conventional and differential mode (Thorlabs DRV504). A piezoelectric

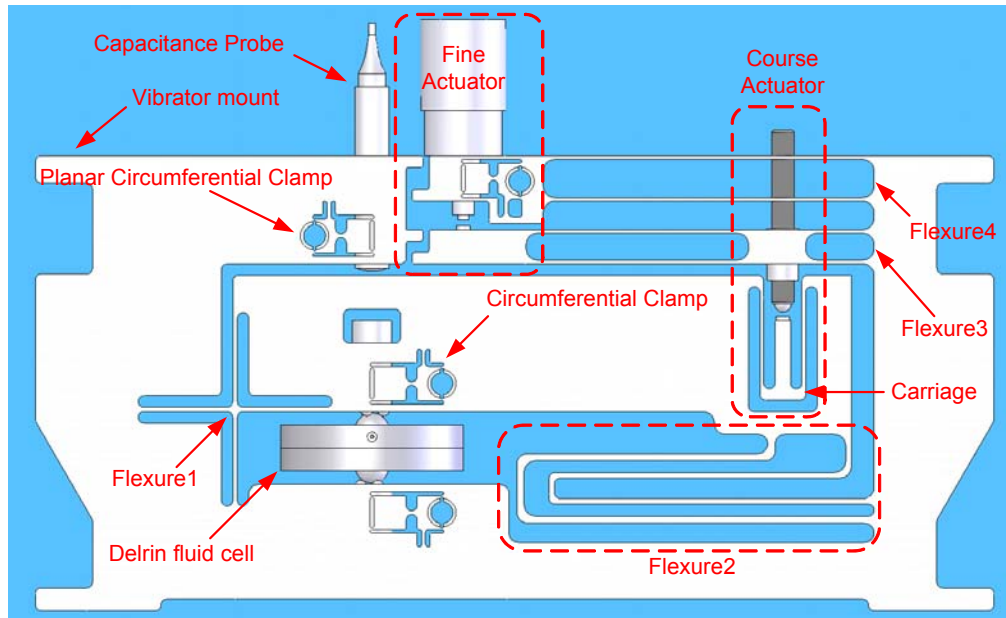


Figure 2: Flexure Mechanism

actuator can also be used to achieve fine position control with no hand contact.

The fine actuator is mounted near the tip of flexure 4 and simultaneously deflects both flexures 3 and 4 to produce a large transmission ratio between the actuator to the electrode. The transmission ratio can be precisely tuned by the geometry of flexure 3 and flexure 4. The design of flexure 3 is composed of three regions: compliant double beam flexure, mount for course actuator, and stiff double-beam flexure. By adjusting the relative position of these three sections, transmission ratios from 10 to 1000 can be achieved. Flexure 4 is a compliant double beam flexure that moves in the opposite direction as the flexure 3 to provide an additional enlargement of the transmission ratio. The designed transmission ratio from the fine actuator to the electrode is 1000:1. The position of the differential screw is delineated at 1 μ m intervals which translate to 1nm delineations through the flexural transmission.

Position Measurement

The position of the cantilever beam is measured using a Lion precision capacitive probe mounted in the flexure. The entire experimental apparatus is encased in a form box in order to minimize measurement drift caused by temperature fluctuations and air currents. Drift studies has shown measurement stability of better than 5nm per hour.

Planar Circumferential Clamp

The sample mount, both actuators, and capacitive position sensors are all cylindrical and are fixed in the flexure by flexure-based circumferential clamps as highlighted in Figure 2. The mechanism of the circumferential clamp can be separated into three parts: the clamp, the expander, and the hour glass flexure. The clamp is half a cylindrical surface which is made to press onto the desired cylinder. The expander is a 1/16" tapered pipe thread which deflects the cylindrical surface when a set screw is advanced into the hole. The hour-glass flexure provides the necessary flexibility in order to accommodate angular misalignment between the clamp and the clamped surface.

Mechanical Drift

A common problem with precision mechanisms that use leads screws in their structural loop is that residual displacement in the backlash of the screw mechanism can relax very slowly, causing a slow positional drift. One remedy for this problem is to add random mechanical energy to expediate the relaxation process. Mechanical vibration is introduced in this flexure by attaching a piezoelectric motor (Newfocus: 8302) to the flexure body. By controlling the speed of the piezoelectric motor, vibration energy can be generated at a precisely controlled frequency.

Electrode Mount

The position of each spherical electrode in the flexure is set by three smaller balls that forms a kinematic tripod mount. The three ball set is

press fitted into a 7/16" post held in the flexure by a circumferential clamp.

Fluidic Cell

The fluid cell is designed to encapsulate the sample fluid in the region between the two spherical electrodes while allowing the electrode separation to be varied. Additional functional requirements include making an electrical contact to the electrodes and minimizing dead volume.

The fluid cell is composed of two identical Delrin discs assembled together with an o-ring seal to form an enclosed chamber. The Delrin discs act as diaphragm flexures that allow the two balls to move with respect to each other. The ball electrodes are mounted at the center of each Delrin disc where a hole allows a small region of the ball to come in contact the fluid. A spherical surface with a matching diameter as the ball is machined into the Delrin disc. By applying an adhesive to this surface, a fluid seal can be produced between the ball and Delrin. Electrical contact to the electrode ball is made via a small recess in the Delrin disc where a wire can be trapped as the ball is inserted into position. Fluid connections in and out of the fluid cell are connected by 6-40 thread flangeless fittings (Upchurch: M-644-03) which adapts 1/16" tubing to the fluid cell.

EXPERIMENTAL VERIFICATION

Preliminary verification of the variable nanometer electrode gap is performed by measuring the capacitance between the electrodes in air. An exact expression for the capacitance between two spheres, C_{ss} , can be obtained from the well-known, but complex, series expression [8]:

$$C_{ss} = 2\pi\epsilon R \sinh(\alpha) \sum_{n=1}^{+\infty} 1/\sinh(n\alpha)$$

where $\cosh(\alpha) = 1 + d/2R$; ϵ is the permittivity of the intervening material; R is the radius of the sphere, and d is the separation between the two closest points on the spheres. An approximate solution was developed by Boyer *et al* [8] for the case where the spheres are very close together, *i.e.*, $d/2R \ll 1$. The expression is then,

$$C_{ss} \approx \pi\epsilon R [\ln(2R/d) + c],$$

where $c \approx 1.843$.

The measured capacitance values obtained using the apparatus of Figure 2 are plotted in

Figure 3 along with Boyer's approximate model. The value of c has been adjusted to obtain the best possible fit. Experimental values deviates slightly from the model at very small gaps and larger gaps. In very small gaps, this deviation is most likely attributed to surface roughness of the electrodes as discussed by Boyer [8]. In larger gaps, this deviation is most likely attributed higher order terms neglected by the small electrode gap approximation.

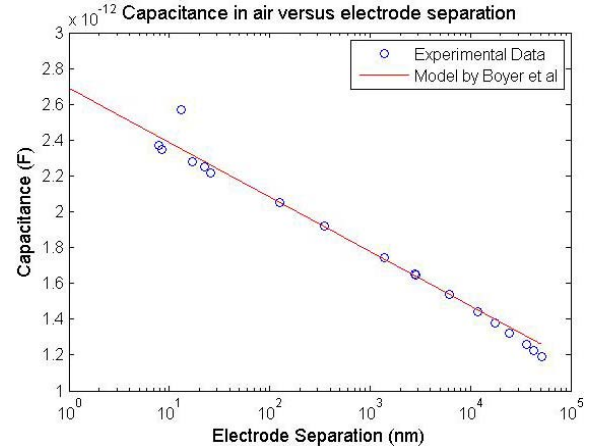


Figure 3: Experimental and theoretical values of capacitance between two spheres in air

ACKNOWLEDGEMENTS

This work has been supported by MIT's Center for Bits and Atoms under NSF Grant CCR0122419. The authors would like to acknowledge Mark Belanger for fabrication assistance.

REFERENCES

- 1 Bazant, M.Z., Chu, K.T., and Bayly, B.J., *SIAM J. Appl. Math.*, 65, 5. (2005)
- 2 Yi, M., K. H. Jeong, and L. P. Lee, *Biosensors and Bioelectronics*, 20 (2005)
- 3 Oh, S., Lee, J.S., Jeong, K.H., Lee, L.P., *Proceedings of IEEE MEMS2003*. (2003)
- 4 Lefebvre, J., Radosavljevic, M., Johnson, A.T., *Appl. Phys. Lett.*, 76, 25. (2000)
- 5 Kanda, A., Wada, M., Hamamoto, Y., Ootuka, Y., *Physica E*, 29. (2005)
- 6 Reed, M. A., C. Zhou, C. J. Muller, T. P. Burgin, Tour, J. M., *Science*, 278, 252. (1997)
- 7 White, J.R., Ma, H., Lang, J., Slocum, A.H., *Rev. Sci. Inst.*, 74, 11. (2003)
- 8 Boyer, L., Houze, F., Tonck, A., Loubet, J.L., Geores, J.M., *J. Phys. D – Appl. Phys.*, 27, 7. (1994)